Available online at www.sciencedirect.com
SCIENCE DIRECT®
Coordination Chemistry Reviews 245 (2003) 191–201
COORDINATION CHEMISTRY REVIEWS
www.elsevier.com/locate/ccr

Review

Catechol oxidase activity of dicopper complexes with N-donor ligands☆

Katalin Selmeczi[a,c], Marius Réglier[c], Michel Giorgi[c], Gábor Speier[a,b,*]

[a] *Research Group for Petrochemistry, Hungarian Academy of Sciences, 8200 Veszprém, Hungary*
[b] *Department of Organic Chemistry, University of Veszprém, Wartha V.u.l., 8200 Veszprém, Hungary*
[c] *Chimie, Biologie et Radicaux Libres, Faculté des Sciences et Techniques de Saint-Jérôme, Université d'Aix-Marseille III, UMR CNRS 6517, Case 432, Avenue Escadrille Normandie-Niemen, 13397 Marseille Cedex 20, France*

Received 20 January 2003; accepted 8 August 2003

Contents

Abstract

The catecholase activity of two dicopper(II) complexes $[Cu_2(L^1)(CF_3SO_3)_2(H_2O)_4](CF_3SO_3)_2$ (**1**) and $[Cu_2(L^2O)](CF_3SO_3)](CF_3SO_3)_2$ (**2**) containing the ligands 1,3-bis{*N*,*N*-bis(2-[2-pyridyl]ethyl)}aminopropane (L^1) and 1,3-bis{*N*,*N*-bis(2-[2-pyridyl]ethyl)}amino-2-hydroxypropane (L^2OH) was studied as functional as well as structural models for the type 3 copper enzyme, catechol oxidase. The X-ray structure of **1** in solid form shows a Cu–Cu distance of 7.840 Å, while in **2** the Cu–Cu distance is only 3.699 Å. Complex **1** can have flexible conformations in solution while the other is being fixed by the bridging alkoxo group. The catalytic activity of the complexes **1** and **2** on the oxidation of 3,5-di-*tert*-butylcatechol was determined spectrophotometrically by monitoring the increase of the 3,5-di-*tert*-butyl-*o*-benzoquinone characteristic absorption at 400 nm over time in methanol saturated with O_2 at 25 °C. The complexes were able to oxidize 3,5-di-*tert*-butylcatechol to the corresponding *o*-quinone and hydrogen peroxide. A kinetic treatment of the data based on steady-state treatment and Michaelis–Menten approach was applied. Mechanisms for the catalytic reactions are proposed, which show that with complex **1** copper(I) dioxygen chemistry determines the kinetic scenario, while with complex **2** the reaction follows a Michaelis–Menten type kinetics.

Keywords: Dinuclear copper complexes; Kinetics; Catechol oxidase models; Dioxygen

☆ Supplementary data associated with this article can be found at doi: 10.1016/j.cct.2003.08.002.

* Corresponding author. Tel.: +36-88-422-022/4657; fax: +36-88-427-492.
E-mail address: speier@almos.vein.hu (G. Speier).

0010-8545/$ – see front matter © 2003 Elsevier B.V. All rights reserved.
doi:10.1016/j.cct.2003.08.002

1. Introduction

Copper has been known as an essential bioelement for some time but its biological role(s) has been recognized only in the last decades due to the rapid development of bioinorganic chemistry, a successful interaction between model complexes and protein biochemistry [1–8]. Copper-containing proteins are involved in various processes in living systems. Hemocyanin (O_2 transport), tyrosinase (hydroxylation of monophenols and oxidation of catechols), and catechol oxidase (oxidation of catechols) are classified as type 3 copper proteins and have magnetically coupled binuclear copper(II) centers at their active sites. The structures of oxidized and reduced forms of catechol oxidase from sweet potato were determined by X-ray crystallography [9–11]. Both consist of a binuclear copper center each coordinated by three hystidine nitrogen atoms. In the oxidized form, the two copper(II) centers with a bridging hydroxide group as the fourth ligand in the four-coordinated trigonal pyramide, and the Cu(II)–Cu(II) distance was found as 2.9 Å. In the reduced form, the Cu(I)–Cu(I) length increases to 4.4 Å. A water molecule coordinates to one copper (Cu_A) with a distorted trigonal pyramidal geometry. The other copper (Cu_B) possesses a square planar geometry with one empty coordination site. Catechol oxidase and tyrosinase are accessible to exogeneous ligands [9]. Tyrosinase catalyzes the oxidation monophenols to *o*-diphenols (cresolase activity) and the subsequent oxidation of the catechols to *o*-quinones (catecholase activity). The enzyme plays an important role in the biosynthesis of melanin pigments and other polyphenolic natural products. Due to the mechanistic suggestions the substrate catechol and the dioxygen (peroxide in a μ-η^2:η^2 fashion) is simultaneously bonded to the reduced enzyme. The copper center is believed to have a six-coordinated ligand arrangement with the monodentate substrate in axial position in a distorted octahedral coordination. Two electrons are transferred from the substrate to the peroxide in the ternary enzyme–catechol–dioxygen complex. This is followed by protonation of the peroxide group and cleavage of the O–O bond accompanied by the loss of water and oxidation of catechol to *o*-quinone. Protonation of the bridging group by the solvent ends up in the resting hydroxide-bridged dicopper(II) state. The Cu(II)–OH–Cu(II) state can be reduced by a further molecule of catechol back to the dicopper(I) oxidation state just closing up the catalytic cycle.

There is a steady interest to investigate the catechol oxidase activity of copper complexes using 3,5-di-*tert*-butylcatechol ($DTBCH_2$) as a convenient model substrate. They can serve as functional mimics for catechol oxidases or as new biomimetic catalysts for oxidation reactions [12–30]. On the basis of structural information and the proposed catalytic mechanisms available for catechol oxidase and tyrosinase, we set ourselves the goal of the synthesis of new model compounds and their use as catalyst in the reaction of 3,5-di-*tert*-butylcatechol with molecular oxygen. There is a view that a close proximity between the two copper centers is a must in the enzyme as well as in model systems [31]. However, mononuclear copper complexes were also shown to be active in model studies for this reaction [32,33]. In this study, we prepared dicopper complexes with the ligands 1,3-bis{*N*,*N*-bis(2-[2-pyridyl]ethyl)}aminopropane (L^1) and 1,3-bis{*N*,*N*-bis(2-[2-pyridyl]ethyl)}amino-2-hydroxypropane (L^2OH). L^1 allows the dicopper complex high flexibility in terms of the Cu–Cu distance, where in the case of the dicopper complex with the ligand L^2OH the bridging alkoxo group behaves as a rigid spacer fixing the Cu–Cu distance. We intended to see what the differences in the interatomic Cu–Cu distances will be, and first of all, what effect this would exert on the mechanism of the aerobic oxidation of 3,5-di-*tert*-butylcatechol in solution (Eq. (1)).

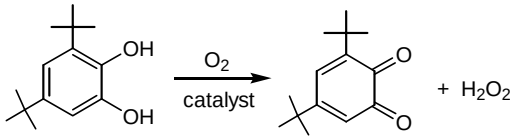

(1)

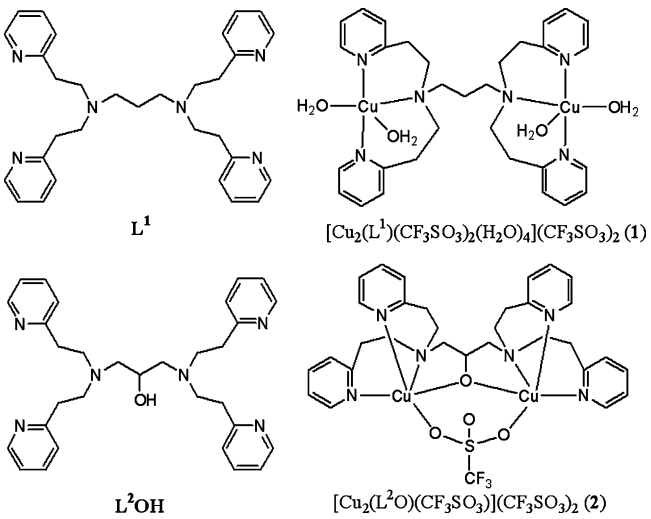

Formulae of the ligands and complexes **1** and **2**

2. Experimental

2.1. Materials and methods

Solvents used for the reactions were purified using literature methods [34]. Commercial starting materials were used without purification, except for 2-vinylpyridine which was chromatographed on silica gel prior to use. 3,5-Di-*tert*-butylcatechol [35], 3,5-di-*tert*-butyl-1,2-benzoquinone [36] were prepared by literature methods. The ligand L^2OH was also prepared by a literature procedure [37]. NMR spectra were recorded at 25 °C in $CDCl_3$ on a

Bruker AC-300 spectrometer. Chemical shifts are reported in ppm as δ values downfield from an internal standard of TMS. Infrared spectra were measured in neat film or KBr pellets on a Specord M80 (Carl Zeiss Jena) and Avatar 330 FT-IR Thermo Nicolet instruments. UV-Vis absorption spectra were recorded on a Shimadzu UV-120A spectrometer. Voltametric analyses were carried out in a standard three-electrode cell using a BAS CV-1B unit. The reference electrode was a AgCl/Ag electrode. The electrolyte consisted of 0.1 M nBu$_4$NClO$_4$ solution in methanol. The auxiliary electrode and the working electrode were platinum. Elemental analyses were measured on C, H, N, S Carlo Erba EA 1108 analyzer. Magnetic susceptibilities were determined at room temperature with a Bruker B-E 10B8 magnetic balance.

2.2. Syntheses

2.2.1. 1,3-bis{N,N-bis(2-[2-Pyridyl]ethyl)}amino-2-hydroxypropane (L^2OH)

1,3-Diamino-2-hydroxypropane (900 mg, 10 mmol) and 2-vinylpyridine (16.8 g, 160 mmol) were heated under reflux in 50 ml of MeOH with acetic acid (3 g, 49 mmol) for 5 days. Methanol was evaporated under vacuum. The resulting brown mixture was taken up in CH_2Cl_2, washed 2× 40 ml of 15% aqueous NaOH and extracted with 2× 30 ml of CH_2Cl_2. The organic layer was dried over Na_2SO_4. The solvent was removed by rotary evaporation to give a crude oil. This oil was dried under vacuum (∼0.01 mmHg) at 40 °C to remove the excess 2-vinylpyridine. The residue was chromatographed on silica gel (CH_2Cl_2/MeOH, 85/15) to yield the pure ligand (yield 31%). ^{1}H NMR ($CDCl_3$), δ (ppm): 2.45 (m, 4H), 2.75–3.0 (m, 16H), 3.40 (s, 1H, OH), 3.60 (m, 1H), 6.90–7.10 (m, 8H), 7.50 (td, $J = 7.5$ Hz, $J = 1.7$ Hz, 4H), 8.40 (dd, $J = 4.0$ Hz, $J = 0.7$ Hz, 4H). ^{13}C NMR ($CDCl_3$), δ (ppm): 35.8 (CH_2), 54.5 (CH_2), 59.0 (CH_2), 66.5 (CH), 121.2 (py CH), 123.5 (py CH), 136.4 (py CH), 149.1 (py CH), 160.5 (py C). IR (neat film), cm^{-1}: 3400 (ν_{O-H}), 3070, 3010 ($\nu_{C-H\ aromatic}$), 2940 ($\nu_{as,C-H\ aliphatic}$), 2820 ($\nu_{s,C-H\ aliphatic}$), 1640, 1600, 1485, 1440 ($\nu_{C-C\ pyridine}$), 1050 (ν_{C-OH}), 770, 756 ($\gamma_{C-H\ aromatic}$, γ_{C-C}). UV-Vis (MeOH), λ_{max} (nm) (ε_{max} (M^{-1} cm^{-1})): 230 (8500) sh, 262 (15,200).

2.2.2. 1,3-bis{N,N-bis(2-[2-Pyridyl]ethyl)}aminopropane (L^1)

A procedure identical to that described for L^2OH was followed for the preparation of this compound. The obtained material was chromatographed on silica gel (CH_2Cl_2/MeOH, 85/15) to yield the pure L^1 (yield 51%). ^{1}H NMR ($CDCl_3$), δ (ppm): 1.55 (qv, $J = 7.0$ Hz, 2H), 2.50 (t, $J = 7.0$ Hz, 4H), 2.8–3.0 (m, 16H), 7.0–7.20 (m, 8H), 7.50 (td, $J = 7.7$ Hz, $J = 1.8$ Hz, 4H), 8.40 (dd, $J = 4.0$ Hz, $J = 0.7$ Hz, 4H). ^{13}C NMR ($CDCl_3$), δ (ppm): 25.0 (CH_2), 35.3 (CH_2), 51.4 (CH_2), 53.3 (CH_2), 120.5 (py CH), 122.8 (py CH), 135.6 (py CH), 148.6 (py CH), 160.1 (py C). IR (neat film), cm^{-1}: 3070, 3010 ($\nu_{C-H\ aromatic}$), 2950 ($\nu_{as,C-H\ aliphatic}$), 2815 ($\nu_{s,C-H\ aliphatic}$), 1640, 1590, 1475, 1440 ($\nu_{C-C\ pyridine}$), 760, 745 ($\gamma_{C-H\ aromatic}$, γ_{C-C}). UV-Vis (MeOH), λ_{max} (nm) (ε_{max} (M^{-1} cm^{-1})): 230 (8550) sh, 262 (15,700).

2.2.3. $[Cu_2(L^2O)(CF_3SO_3)](CF_3SO_3)_2$ (2)

Ligand L^2OH (510 mg, 1 mmol) solubilized in CH_2Cl_2 (5 ml) was dropwise added to a suspension of $Cu(CF_3SO_3)_2$ (723.4 mg, 2 mmol) in CH_2Cl_2 (5 ml). After 2 h stirring at room temperature, a green-blue solid was formed. This copper(II) complex $[Cu_2(L^2O)(CF_3SO_3)](CF_3SO_3)_2$ was filtered, washed with Et_2O and dried under vacuum. Yield: 1.12 g, 91%. IR (KBr), cm^{-1}: 3080 ($\nu_{C-H\ aromatic}$), 2980 ($\nu_{as,C-H\ aliphatic}$), 2820 ($\nu_{s,C-H\ aliphatic}$), 1660, 1610, 1490, 1455 ($\nu_{C-C\ pyridine}$), 775, 760 ($\gamma_{C-H\ aromatic}$, γ_{C-C}), 1285, 1034, 641, 526 ($\nu_{CF_3SO_3^-}$). UV-Vis (MeOH), λ_{max} (nm) (ε_{max} (M^{-1} cm^{-1})): 215 (9100), 260 (15800), 382 (1350), 685 (280). $C_{34}H_{37}N_6Cu_2O_{10}F_9S_3$ (1083.08): calcd. C 37.67, N 7.75, H 3.41, Cu 11.73; found C 37.12, N 7.43, H 3.19, Cu 12.05. $\mu_{eff} = 1.35$ BM/Cu.

2.2.4. $[Cu_2(L^1)(CF_3SO_3)_2(H_2O)_4](CF_3SO_3)_2$ (1)

This copper(II) complex was prepared analogously to $[Cu_2(L^2O)(CF_3SO_3)](CF_3SO_3)_2$. Yield: 1.0 g, 82%. IR (KBr), cm^{-1}: 3100 ($\nu_{C-H\ aromatic}$), 2980 ($\nu_{as,C-H\ aliphatic}$), 2870 ($\nu_{s,C-H\ aliphatic}$), 1660, 1620, 1500, 1450 ($\nu_{C-C\ pyridine}$), 775, 740 ($\gamma_{C-H\ aromatic}$, γ_{C-C}) 1275, 1034, 630, 516 ($\nu_{CF_3SO_3^-}$). UV-Vis (MeOH), λ_{max} (nm) (ε_{max} (M^{-1} cm^{-1})): 215 (10400), 260 (16800), 370 (2400) sh, 670 (280). $C_{35}H_{46}N_6O_{16}F_{12}S_4Cu_2$ (1290.1): calcd. C 32.55, N 6.50, H 3.56, Cu 9.85; found C 33.0, N 6.60, H 3.31, Cu 10.55. $\mu_{eff} = 1.55$ BM/Cu.

2.3. X-ray structure determination

Crystallographic and experimental details of the data collection and refinement of the structure of $[Cu_2(L^2O)(CF_3SO_3)](CF_3SO_3)_2$ (**2**) and $[Cu_2(L^1)(CF_3SO_3)_2(H_2O)_4](CF_3SO_3)_2$ (**1**) are reported in Table 1. All measurements were performed on a Bruker-Nonius Kappa CCD diffractometer using graphite monochromated Mo Kα radiation [38]. The cells determinations and data integrations were performed using Denzo-Scalepak [39]. The structure solutions were obtained using Sir92 [40] and the refinements were done by SHELXL-97 [41].

2.4. Cyclic voltammetry

All experiments were run at room temperature under argon atmosphere. The complexes (0.5 mM) were dissolved in MeOH containing (0.1 M) tetrabutylammonium perchlorate (TBAP) as the supporting electrolyte. The cyclic voltammograms were recorded at a platinum working electrode (1.6 mm disk) with saturated AgCl/Ag reference electrode and Pt wire as an auxiliary electrode.

Table 1
Crystallographic data for the complexes $[Cu_2(L^1)(CF_3SO_3)_2(H_2O)_4](CF_3SO_3)_2$ (**1**) and $[Cu_2(L^2O)(CF_3SO_3)](CF_3SO_3)_2$ (**2**)

	$[Cu_2(L^1)(CF_3SO_3)_2(H_2O)_4](CF_3SO_3)_2$	$[Cu_2(L^2O)(CF_3SO_3)](CF_3SO_3)_2$
Formula	$C_{35}H_{46}Cu_2F_{12}N_6O_{16}S_4$	$C_{34}H_{37}Cu_2F_9N_6O_{10}S_3$
Crystal system	Monoclinic	Orthorhombic
Space group	$P2_1/m$	*Pnma*
a (Å)	7.9636(3)	16.9950(2)
b (Å)	28.442(1)	23.2200(2)
c (Å)	11.7137(7)	11.0680(4)
β (°)	103.850(3)	
V (Å)	2576.2(2)	4367.7(2)
Z	2	4
$d_{calcd.}$ (g cm^{-3})	1.581	1.815
Crystal color/size (mm^3)	Blue/0.4 × 0.2 × 0.2	Green/0.4 × 0.4 × 0.2
μ(Mo Kα) (cm^{-1})	1.090	1.5
F(0 0 0)	1248	2496
T (K)	293	293
Scan mode	ϕ scan	ϕ scan
Data collected	4840	6800
Parameters	368	349
R	0.0869	0.0682
wR	0.2344	0.1691
S	1.045	1.042
$\Delta\rho_{max}$ (eÅ^3)	1.137	0.608
$\Delta\rho_{min}$ (eÅ^3)	−0.940	−0.961

(**1**) R: $F^2 > 4\sigma F^2$; wR: $w = 1/[\sigma^2(F_o^2) + (0.1483P)^2 + 5.6669P]$, where $P = (F_o^2 + 2F_c^2)/3$. (**2**) R: $F^2 > 4\sigma F^2$; wR: $w = 1/[\sigma^2(F_o^2) + (0.0879P)^2 + 7.2258P]$, where $P = (F_o^2 + 2F_c^2)/3$.

2.5. Kinetics of 3,5-di-tert-butylcatechol oxidation

The oxidation of 3,5-di-*tert*-butylcatechol was performed under pseudo-first-order conditions in a thermostatically controlled reaction vessel connected to a mercury manometer to maintain a constant pressure. The temperature during the measurement was kept constant at 25 ± 0.1 °C and was varied from 20 to 38 °C for determination of the activation parameters. The solvent employed was methanol saturated with dioxygen or with mixture dioxygen–argon (0–80% of O_2) in different ratios. The dioxygen concentration in methanol at 25 °C as 1.02×10^{-2} M was applied and was varied from 0.35 to 1.03×10^{-2} M in the 20–38 °C temperature range according to literature data [42]. The concentration of the copper complexes was varied from 0.6×10^{-4} to 5.0×10^{-4} M while that of substrate from 1.25×10^{-3} to 18.7×10^{-3} M. The absorption at $\lambda_{max} = 400$ nm ($\varepsilon = 1560\ M^{-1}\ cm^{-1}$) characteristic of the formed quinone was measured as a function of time. The hydrogen peroxide formation during the catalytic reaction was determined by iodometric titration [43].

3. Results and discussion

3.1. X-ray structures

Single crystals of $[Cu_2(L^1)(CF_3SO_3)_2(H_2O)_4](CF_3SO_3)_2$ (**1**) suitable for X-ray structure determination were grown from MeOH. It crystallized in a monoclinic space group $P2_1/m$ and crystallographic data are compiled in Table 1. The structure of **1** (Fig. 1) consists of a discrete binuclear complex with two trigonal bipyramidally coordinated Cu(II) ions. The two copper atoms are related by a crystallographic mirror plane containing C17, S1, S2, C18 of the two triflate groups as well as C16 of the connecting methylene chain in L^1. The coordination geometry around the copper atoms is slightly distorted trigonal bipyramidal with a τ value of 0.96. Addison et al. defined $\tau = 1$ for a regular trigonal bipyramide, while $\tau = 0$ denotes a regular square pyramide

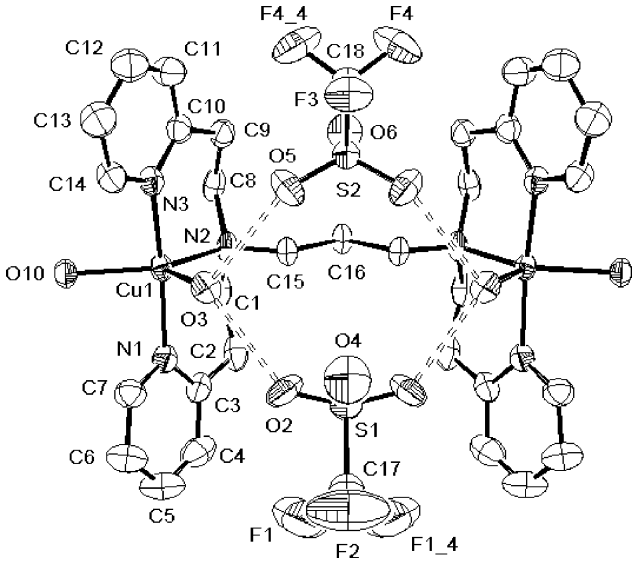

Fig. 1. The molecular structure of $[Cu_2(L^1)(CF_3SO_3)_2(H_2O)_4](CF_3SO_3)_2$ (**1**).

[44]. The values of τ between these limits denote the degree of bipyramidicy. The two pyridine nitrogen atoms occupy axial positions with the bond distances Cu1–N1 1.993(5) Å and Cu1–N3 1.984(5) Å and a N1–Cu1–N3 angle of 167.3(2)°. These bond lengths are somewhat shorter than those found for the dicopper(I) carbonyl complex $Cu_2(L^1)(CO)_2(ClO_4)_2$ (2.023(8) and 2.040(10) Å) [37]. The equatorial positions are occupied by the aliphatic N atom of the ligand L^1 with a Cu1–N2 distance of 2.023(4) Å and two O atoms from coordinated water molecules. One of the water molecules is hydrogen bonded to the oxygen atoms of two $CF_3SO_3^-$ molecules with a O3–O5 and O3–O2 bond distances of 2.848 and 2.700 Å, respectively. The copper–oxygen distance (Cu1–O3) with the in H-bonding involved H_2O molecule is 2.226(4) Å, while that of the other water molecule is shorter (Cu1–O10 2.076(4) Å). The equatorial Cu1–N2 distance (2.023(4) Å) is somewhat longer than those of the axial copper–nitrogen distances (Cu1–N1 1.993(5) Å, Cu1–N3 1.984(5) Å). The copper–copper distance (7.840 Å) is rather large in the solid state. This may be fixed through the hydrogen bridged entities of the two equatorial water molecules and the two $CF_3SO_3^-$ anions involved. However, it must be kept in mind that different situations can probably be considered in solution, since in solution the H-bridged system may be broken down, the $CF_3SO_3^-$ anions may be dissociated and then the dicopper complex can have various conformations due to the flexibility of the methylene bridge between the two aliphatic N-atoms. The most important interatomic bond distances and angles are compiled in Table 2.

From the complex $[Cu_2(L^2O)(CF_3SO_3)](CF_3SO_3)_2$ (**2**) suitable crystals were obtained by slow diffusion of ether into the CH_2Cl_2 solution of **2**. It crystallized in the orthorhombic space group *Pnma* and crystallographic data can be found in Table 1. The molecular structure of $[Cu_2(L^2O)(CF_3SO_3)](CF_3SO_3)_2$ (**2**), as shown in Fig. 2, also consists of a discrete binuclear complex with two

Table 2
Selected interatomic distances (Å) and angles (°) of the complexes $[Cu_2(L^1)(CF_3SO_3)_2(H_2O)_4](CF_3SO_3)_2$ (**1**) and $[Cu_2(L^2O)(CF_3SO_3)](CF_3SO_3)_2$ (**2**)

Distances (Å)		Angles (°)	
$[Cu_2(L^1)(CF_3SO_3)_2(H_2O)_4](CF_3SO_3)_2$ (**1**)			
Cu1–N1	1.993(5)	N3–Cu1–N1	167.3(2)
Cu1–N2	2.023(4)	N3–Cu1–N2	95.8(2)
Cu1–N3	1.984(5)	N1–Cu1–N2	95.5(2)
Cu1–O3	2.226(4)	N2–Cu1–O3	109.95(16)
Cu1–O10	2.076(4)	N2–Cu1–O10	130.77(17)
Cu1–Cu2	7.840(4)	O10–Cu1–O3	119.28(17)
		N1–Cu1–O10	87.84(18)
		N3–Cu1–O10	89.04(18)
		N1–Cu1–O3	86.79(19)
		N3–Cu1–O3	84.04(19)
$[Cu_2(L^2O)(CF_3SO_3)](CF_3SO_3)_2$ (**2**)			
Cu1–N1	2.032(3)	N1–Cu1–N3	98.93(14)
Cu1–N2	2.009(3)	N2–Cu1–N3	95.40(10)
Cu1–N3	2.179(4)	O1–Cu1–N3	104.69(11)
Cu1–O1	1.969(12)	O2–Cu1–N3	95.71(16)
Cu1–O2	2.047(3)	N2–Cu1–O2	83.10(13)
Cu1–Cu2	3.699(3)	N2–Cu1–N1	94.17(12)
		O1–Cu1–N1	87.04(12)
		O1–Cu1–O2	90.54(12)
		N1–Cu1–O2	165.31(15)
		O1–Cu1–N2	159.45(14)
		Cu1–O1–Cu2	139.82(18)

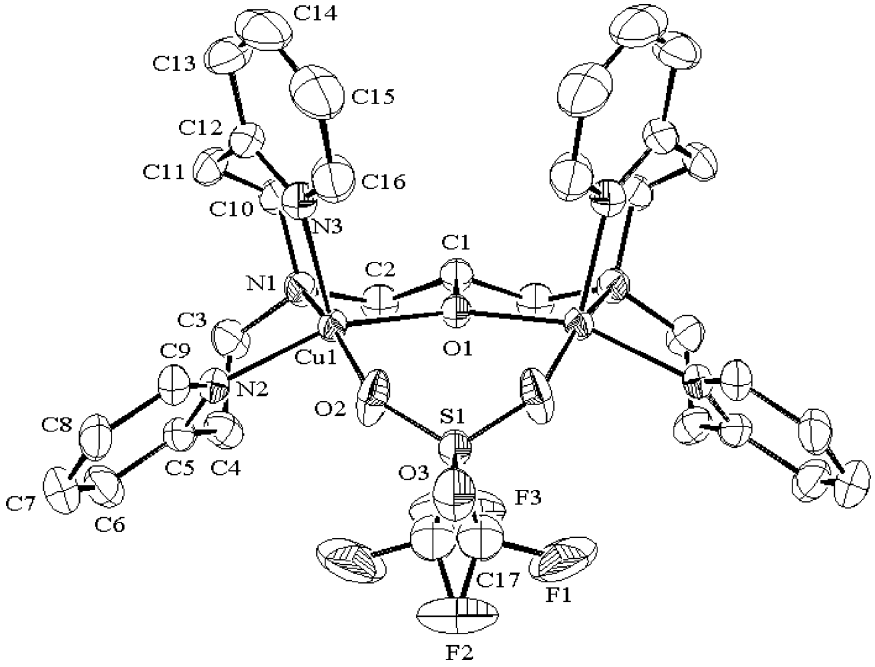

Fig. 2. The molecular structure of $[Cu_2(L^2O)(CF_3SO_3)](CF_3SO_3)_2$ (**2**).

tetragonally coordinated Cu(II) ions bridged in the equatorial positions by the alkoxide and triflate ligands. The τ value of 0.11 of the complex also expresses slight distortion of a regular square pyramid [44]. The two copper atoms are related by a crystallographic mirror plane containing the O1, C1, S1, and C17 atoms of the ligand L^2O and the triflate. The Cu–Cu distance was found to be 3.699(3) Å. This is somewhat shorter than that found, e.g. in the similar $[Cu_2(L^2O)(OMe)](PF_6)_2$ (2.995(2) Å) [45]. The two positions in the basal plane of the copper ions are taken by one of the pyridine nitrogen ligands and the aliphatic nitrogen of the ligand L^2OH. The other two equatorial positions are occupied by the oxygen atoms O1 of the ligand L^2OH and O2 of the triflate anion. In the distorted square pyramidal dicopper complex, the out of plane distance of the basal plane atoms O1, O2, N1, N2 is 0.045 Å while that involving Cu1 as well is 0.127 Å. The axial pyridine N3 donor which is bonded to the Cu(II) atom at a distance of 2.179(4) Å, is a bit longer than the equatorial pyridine donor N2 (Cu1–N2 2.009(3) Å). The whole feature of bond distances, bond angles of **2** (Table 2) show similarities to other dicopper complexes with ligands derived from 2-hydroxy-1,3-diaminopropane [45–47].

3.2. Electrochemistry

The electrochemistry of the complexes was investigated, as the redox potential is an important parameter in electron transfer processes in general and also in our catalytic systems. The redox potentials of the catalysts and species involved in the redox cycles have to match some criteria. The reduction of Cu(II) by the substrate $DTBCH_2$ and the reoxidation of Cu(I) by dioxygen are significant steps in the catalytic cycle. The reduction potentials for the complexes **1** and **2** were measured by cyclic voltammetry (CV) at a working platinum electrode in methanol solution containing 0.1 M TBAP as the supporting electrolyte in the range of −1.0 to 1.2 V versus AgCl/Ag. The cyclic voltammograms of **1** and **2**, as shown in Fig. 3, do not show reversible peaks.

The reduction potentials of **1** at 380 and −60 mV versus the AgCl/Ag (the redox potential of AgCl/Ag was taken as 45 mV more negative than the SCE [48]), which can be assigned to $Cu^{II}Cu^{II} \rightarrow Cu^{II}Cu^{I}$ and $Cu^{II}Cu^{I} \rightarrow Cu^{I}Cu^{I}$ processes. In the case of **2**, only one reduction peak at 60 mV versus AgCl/Ag could be seen. In both cases the complexes exhibit a sharp anodic oxidation peak in the range of 400–440 mV versus AgCl/Ag, probably corresponding to a process involving Cu^0 at the electrode surface. These reduction potentials, however, do differ the reported value of +360 mV versus SCE for the enzyme tyrosinase isolated from mushrooms [49].

3.3. Spectroscopic properties

The electronic spectra of the complexes **1** and **2** recorded in MeOH solution exhibit, besides the intense UV absorptions below 300 nm, due to pyridine π–π^* transitions, poorly defined adsorptions of moderate intensities between 300 and 400 nm, which can be attributed to σ(amino) → Cu(II) [50] and π(pyridine) → Cu(II) [51,52] LMCT transitions. In addition, two weaker and partially resolved bands can be found in the visible region near 685 and 670 nm. The presence of the d–d bands in this region is consistent with coordination geometries close to trigonal bipyramidal for the Cu(II) center bound to three nitrogen and two oxygen donors and to square pyramidal for the Cu(II) center bound three nitrogen donors and the bridging alkoxide and triflate oxygen atoms [53]. The absorptions at 382 and 370 nm in the visible region are much lower in energy than those found in other RO-bridged dicopper complexes [54–57]. However, in many cases alkoxo bridged dicopper complexes do not exhibit any absorptions due to CT bands having either imidazole, pyrazolate or pyridine ligands.

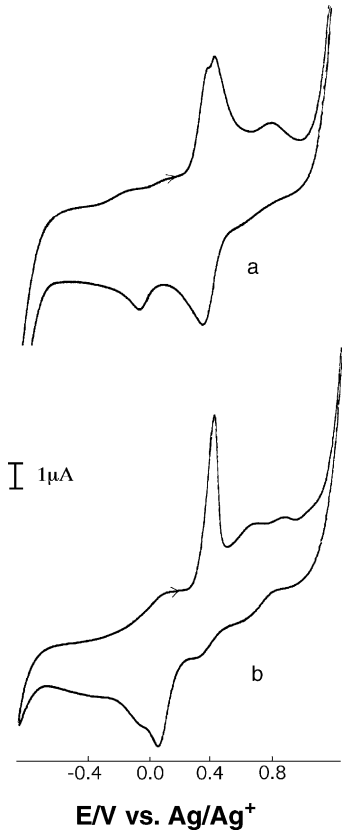

Fig. 3. The cyclic voltammograms of the complexes $[Cu_2(L^1)(CF_3SO_3)_2(H_2O)_4](CF_3SO_3)_2$ (**1**) (a) and $[Cu_2(L^2O)(CF_3SO_3)](CF_3SO_3)_2$ (**2**) (b) in MeOH. Concentration of **1** and **2**: 5×10^{-3} M in MeOH (0.1 M Bu_4NClO_4); sweep rate = 100 mV s^{-1}; AgCl/Ag reference electrode.

The EPR spectra recorded in MeOH solution at room temperature showed that in the complex $[Cu_2(L^2O)(CF_3SO_3)](CF_3SO_3)_2$ (**2**) no signal could be seen due to strong antiferromagnetic spin coupling of the two Cu(II) centers. The solid state magnetic susceptibility of this compound (μ_{eff} = 1.35 BM/Cu) supports this behavior. Compound **1** also showed

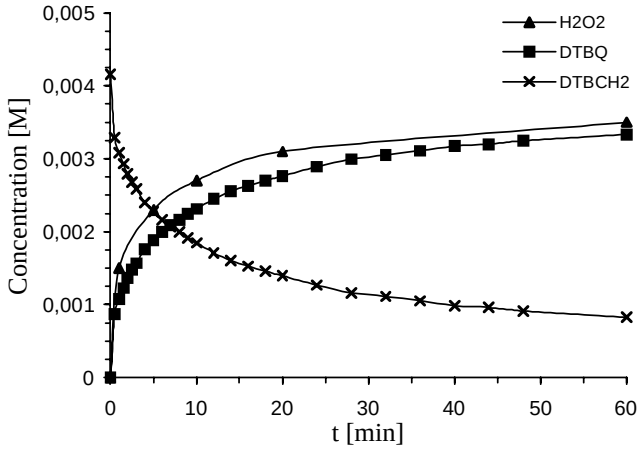

Fig. 4. The oxidation of $DTBCH_2$ catalyzed by $[Cu_2(L^1)(CF_3SO_3)_2(H_2O)_4](CF_3SO_3)_2$ (**1**). Conditions: $[[Cu_2(L^1)(CF_3SO_3)_2(H_2O)_4](CF_3SO_3)_2] = 0.125$ mM, $[DTBCH_2] = 4.16$ mM, $[O_2] = 10.2$ mM at 25 °C in MeOH.

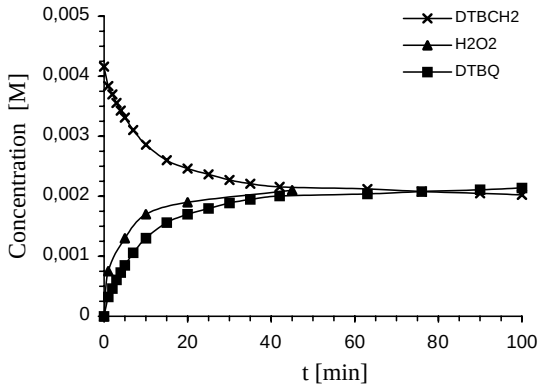

Fig. 5. The oxidation of $DTBCH_2$ catalyzed by $[Cu_2(L^2O)(CF_3SO_3)](CF_3SO_3)_2$ (**2**). Conditions: $[[Cu_2(L^2O)(CF_3SO_3)](CF_3SO_3)_2] = 0.125$ mM, $[DTBCH_2] = 4.16$ mM, $[O_2] = 10.2$ mM at 25 °C in MeOH.

some slight magnetic interaction between the two copper(II) centers ($\mu_{eff} = 1.55$ BM/Cu) but it was EPR-active at room temperature giving a broad signal with the parameters $g_{xx} = 2.252$, $g_{yy} = 2.081$, and $g_{zz} = 2.050$. In CH_2Cl_2, due to decomposition and precipitation of solid copper complexes, no useful solution spectra could be obtained.

3.4. Kinetic studies for catechol oxidase activity

Compounds **1** and **2** are stable under ambient conditions in air. The catechol oxidase activity of the enzyme is carried out by the met form of the enzyme (Cu(II)–Cu(II)) through a two electron-transfer reaction. The catechol oxidase activity of copper complexes, as model systems, has been determined mainly by the catalytic oxidation of $DTBCH_2$ [31,58]. The kinetic studies of the oxidation of $DTBCH_2$ catalyzed by the complexes **1** and **2** were carried out by the initial rate method monitoring the increase of the concentration of 3,5-di-*tert*-butyl-*o*-benzoquinone (DTBQ) at the characteristic band at 400 nm and the amount of hydrogen peroxide formed by iodometric titration over the time. It was found that in the absence of dioxygen no catalytic oxidation of the substrate occurs, however, $DTBCH_2$ is oxidized to DTBQ by Cu(II) in a fast reaction. The ability of Cu(II) to oxidize a large number of organic compounds has already been demonstrated [59]. Dioxygen is necessary in the catalytic reaction and its role is the reoxidation of copper(I) species formed during the catalytic cycle. The time course of the reactions catalyzed by the complexes **1** and **2** is shown in Figs. 4 and 5, and from them it can be seen that under the ambient conditions described, the reactions are ~50% completed in ca. 30 min. No decomposition of the H_2O_2 formed could be observed and the reaction between the quinone DTBQ and hydrogen peroxide is negligible. Furthermore, no other products such as those of a cleavage reaction could be detected. The kinetic experiments of the reactions were conducted under pseudo-first-order conditions (the concentration of dioxygen was kept constant) and at 25 °C in methanol. The absorbance at 400 nm of the DTBQ increases and the Beer–Lambert rule was valid for the various concentrations. Carrying out the kinetic experiments with **1** by varying the concentration of one of the reaction partners and keeping the other two constant, the reaction rate was found to be independent of the $DTBCH_2$ concentration. A first-order dependence was found for the catalyst $[Cu_2(L^1)(CF_3SO_3)_2(H_2O)_4](CF_3SO_3)_2$ (**1**) concentration and the dependence on the dioxygen concentration was found to give a saturation curve as shown in Fig. 6. The kinetic data are compiled in the supplementary material.

On the basis of the kinetic data a mechanism route A as depicted in Scheme 1 is proposed. We believe that the catalyst weighted in as $[Cu_2(L^1)(CF_3SO_3)_2(H_2O)_4](CF_3SO_3)_2$ (**1**) oxidizes $DTBCH_2$ in a fast reaction step (k_1) to the quinone DTBQ and $2H^+$ forming the dicopper(I) species $(Cu^I)_2$ (**3**). This dinuclear copper(I) complex then reacts in a reversible

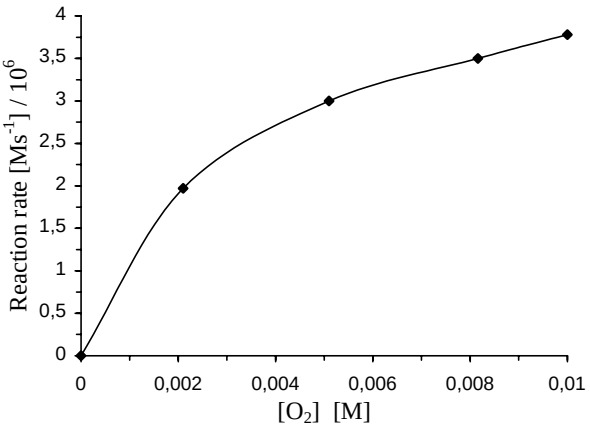

Fig. 6. The dependence of the oxidation rate of $DTBCH_2$ catalyzed by $[Cu_2(L^1)(CF_3SO_3)_2(H_2O)_4](CF_3SO_3)_2$ (**1**) on the dioxygen concentration. Conditions: $[[Cu_2(L^1)(CF_3SO_3)_2(H_2O)_4](CF_3SO_3)_2] = 0.125$ mM, $[DTBCH_2] = 4.16$ mM at 25 °C in MeOH.

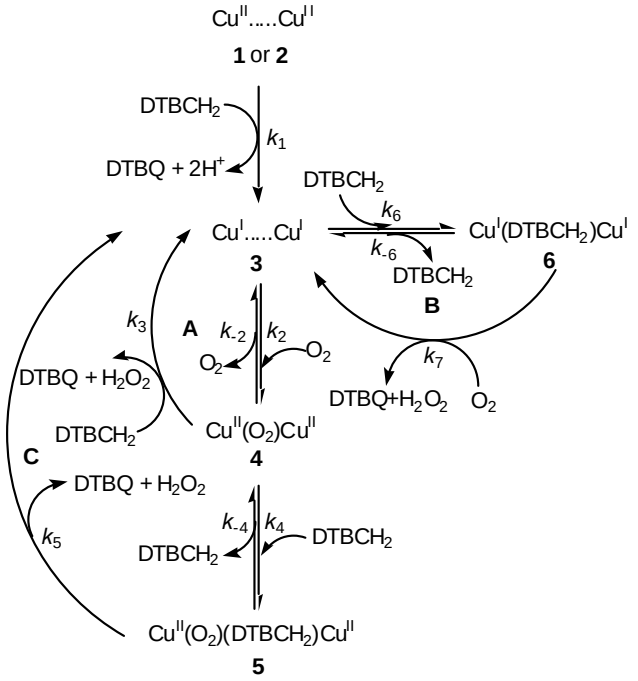

Scheme 1.

reaction with dioxygen in a slow, rate-determining step (k_2) to the copper dioxygen complex $(Cu^{II})_2(O_2)$ (**4**). $(Cu^{II})_2(O_2)$ reacts then with $DTBCH_2$ in a fast reaction step (k_3) to give the products DTBQ and H_2O_2 and the $(Cu^{II})_2(O_2)$ (**4**) is reduced to $(Cu^{I})_2$ (**3**) in closing up the catalytic cycle (route A). In the scheme, we also indicated other possible reaction pathways like that where the dioxygen complex $(Cu^{II})_2(O_2)$ (**4**) reacts with $DTBCH_2$ (k_4) leading to the ternary complex **5** and its reaction (k_5) leads to **3**, DTBQ, and H_2O_2 (route C). Route B would also satisfy the kinetic data if the reaction of $(Cu^{I})_2(DTBCH_2)$ (**6**) with O_2 (k_7) is rate-limiting and k_6 is large. However, we think that these reactions are not significant and their proportion on the whole mechanism does not influence the main kinetic pathway.

Applying steady-state treatment for the reaction assuming that the concentration of $(Cu^{II})_2(O_2)$ (**4**) remains constant during the whole reaction time the rate law (2) can be deduced provided that the k_3 value is of similar order of magnitude as k_{-2}. The corresponding rate constants and activation parameters for the oxidation of $DTBCH_2$ by O_2 catalyzed by **1** are compiled in Table 3.

$$\text{reaction rate} = \frac{k_2[O_2]k_3[DTBCH_2][\mathbf{1}]}{k_{-2} + k_3[DTBCH_2] + k_2[O_2]} \quad (2)$$

The parameters calculated from the rate equation (2) show that the rate-determining reaction step (k_2) is the formation of the dioxygen complex $(Cu^{II})_2(O_2)$ (**4**) from the reduced $(Cu^{I})_2$ complex (**3**). The large negative entropy of activation also confirms a bimolecular elementary step. The rate equation describes well the kinetic parameters and especially the saturation curve in terms of the dioxygen concentration. However, when $(Cu^{I})_2(O_2)$ reacts with $DTBCH_2$ in a fast

Table 3
The rate constants and activation parameters for the oxidation of $DTBCH_2$ catalyzed by the complexes **1** and **2**

Kinetic parameters	**1**	**2**
k_2 ($M^{-1}\,s^{-1}$)	7.6	3.1
k_{-2} (s^{-1})	0.05	1.0×10^{-4}
k_3 ($M^{-1}\,s^{-1}$)		5.3
E_A ($kJ\,mol^{-1}$)	50.2	59.5
$\Delta H^{\ddagger}$ ($kJ\,mol^{-1}$)	47.6	57.0
$\Delta S^{\ddagger}$ ($J\,mol^{-1}$)	−76.0	−6.9
$\Delta G^{\ddagger}$ ($kJ\,mol^{-1}$)	70.3	59.0

step (k_3), the deoxygenation process (k_{-2}) has no opportunity to occur (a first-order dependence with regard to the dioxygen concentration would result), so at low dioxygen concentration the rate equation simplifies to Eq. (3).

$$\text{reaction rate} = k_2[\mathbf{1}][O_2] \quad (3)$$

At higher dioxygen concentration the interplay of the two forms gives the saturation curve and the non-dependence on dioxygen after a certain value of dioxygen concentration.

The catalytic reaction is determined and can be interpreted by, single copper(I) dioxygen chemistry, where the reaction of the dicopper(I) complex with dioxygen is rate-limiting.

The oxidation of $DTBCH_2$ catalyzed by the complex $[Cu^{II}_2(L^2O)(CF_3SO_3)](CF_3SO_3)_2$ (**2**) resulted in the products DTBQ and hydrogen peroxide as well. For the kinetic measurements the initial rate method was chosen under pseudo-first-order conditions (the dioxygen concentration being held constant). A variation of the catalyst concentration by constant dioxygen pressure and substrate concentration gave initial reaction rates which were linear with the catalyst concentration with an R^2 value of 99.6%. A variation of the substrate concentration by constant dioxygen pressure and catalyst concentration showed a saturation

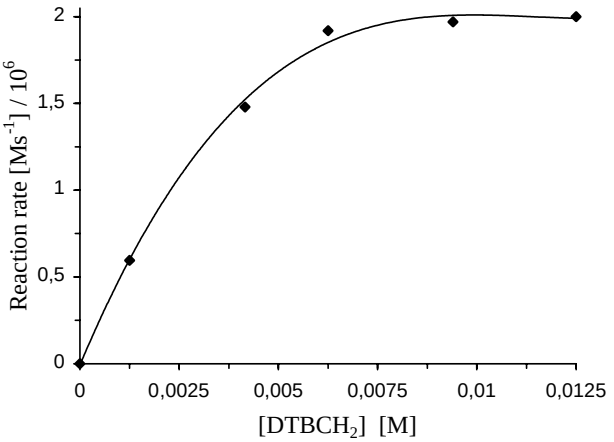

Fig. 7. The dependence of the reaction rate of the aerobic oxidation of $DTBCH_2$ catalyzed by $[Cu_2(L^2O)(CF_3SO_3)](CF_3SO_3)_2$ (**2**) on the substrate concentration. Conditions: $[[Cu_2(L^2O)(CF_3SO_3)](CF_3SO_3)_2] = 0.125$ mM, $[O_2] = 10.2$ mM at 25 °C.

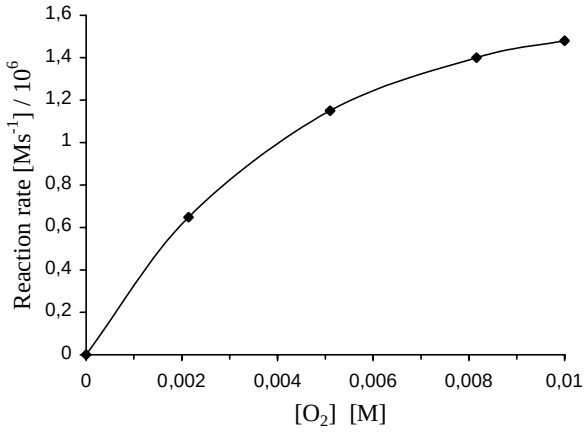

Fig. 8. The dependence of the reaction rate of the aerobic oxidation of $DTBCH_2$ catalyzed by $[Cu_2(L^2O)(CF_3SO_3)](CF_3SO_3)_2$ (**2**) on the dioxygen concentration. Conditions: $[[Cu_2(L^2O)(CF_3SO_3)](CF_3SO_3)_2] = 0.125$ M, $[DTBCH_2] = 4.16$ mM at 25 °C.

curve as shown in Fig. 7. The effect of the dioxygen concentration on the reaction rate again showed a saturation curve as can be seen in Fig. 8.

The reaction followed a Michaelis–Menten type kinetics. The Lineweaver–Burk plot can be seen in Fig. 9. The calculated values for the $K_M = 2.92 \times 10^{-3}$ M, $k_{cat} = 3.28 \times 10^{-2}\ s^{-1}$, and $K_M/k_{cat} = 89.02 \times 10^{-3}$ M s were in the same order of magnitude as found by other dicopper model systems [31,24,60].

An interpretation of the kinetic data can be done on the possible reaction sequences as shown in Scheme 1. There are three reaction pathways which satisfy the kinetics found for the oxidation reaction. Route A assumes the fast irreversible reduction of **2** by $DTBCH_2$ to **3** followed by the formation of the dicopper dioxygen complex **4** in a fast pre-equilibrium, which reacts then with $DTBCH_2$ in the rate-determining step (k_3) to the starting dicopper(I) species **3** and the products

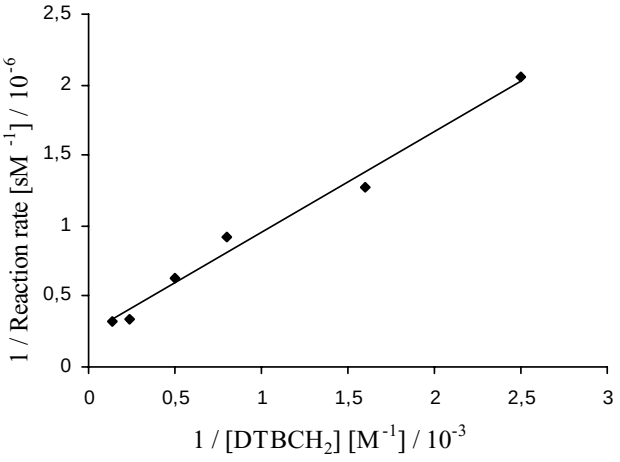

Fig. 9. The Lineweaver–Burk plot for the oxidation of $DTBCH_2$ with dioxygen catalyzed by $[Cu_2(L^2O)(CF_3SO_3)](CF_3SO_3)_2$ (**2**). Conditions: $[[Cu_2(L^2O)(CF_3SO_3)](CF_3SO_3)_2] = 0.125$ mM, $[O_2] = 10.2$ mM at 25 °C.

DTBQ and H_2O_2, respectively. A steady-state treatment for this route assuming $d[Cu^{II}(O_2)Cu^{II}]/dt = 0$ the similar rate law (4) can be deduced. This rate law clearly describes the scenario of the reaction.

$$\text{reaction rate} = \frac{k_2[O_2]k_3[DTBCH_2][\mathbf{2}]}{k_{-2} + k_3[DTBCH_2] + k_2[O_2]} \quad (4)$$

In that case the rate of the reaction is influenced by k_2 and k_3 as well. By curve fitting the following values for the rate constants could be calculated: $k_2 = 2.8\ M^{-1}\ s^{-1}$, $k_{-2} = 0.0001\ s^{-1}$, and $k_3 = 5.3\ M^{-1}\ s^{-1}$, however, we do not believe that this represents the only true situation. Route B in Scheme 1 seems to be also plausible, where the reduced dicopper(I) complex **3** undergoes a fast pre-equilibrium with the substrate $DTBCH_2$ (k_6) to give $(Cu^I)(DTBCH_2)(Cu^I)$ (**6**). This complex reacts then in the rate-limiting step with dioxygen to give the products DTBQ and H_2O_2 (k_7). In route C in two consecutive pre-equilibria (k_2 and k_4) the ternary complex of $(Cu^I)(O_2)(DTBCH_2)(Cu^I)$ (**5**) is formed from **3** in fast reactions and small equilibrium constants. This is converted then in the rate-determining reaction step (k_5) to the complex **3** and the products DTBQ and H_2O_2, respectively. Route B can be ruled out since it disagrees with the observed substrate saturation behavior. Furthermore, addition of $DTBCH_2$ to the oxygenated solution of **3** shows a sudden color change from blue to yellow/brown indicating the reduction of Cu(II) to Cu(I) and the formation of DTBQ. The kinetic and activation parameters are compiled in Table 3. The negative activation of entropy suggests also an associative mechanism for the rate-limiting step.

4. Conclusions

We have synthesized two dicopper complexes with N-ligands. The one with a spacer OH-group and the other without. The X-ray structures of the complexes show that the complex $[Cu_2(L^1)(CF_3SO_3)_2(H_2O)_4](CF_3SO_3)_2$ (**1**) has a flexible structure and a long Cu–Cu distance while that in $[Cu_2(L^2O)(CF_3SO_3)](CF_3SO_3)_2$ with the alkoxo group (**2**) is rather short. In the former, the copper ion has trigonal bipyramidal environment, while in **2**, a square pyramidal geometry around the Cu(II) ions could be found. In complex **1**, there is only a slight magnetic interaction between the two magnetic Cu(II) centers. In **2**, however, an antiferromagnetic interaction between the copper(II) centers decreases the magnetic moment and the complex is EPR-silent. Both complexes are stable under ambient conditions and catalyze the oxidation of 3,5-di-*tert*-butylcatechol to 3,5-di-*tert*-butyl-*o*-benzoquinone and hydrogen peroxide by dioxygen at room temperature and atmospheric dioxygen pressure. Practically no other products are formed in the catalytic reactions and also no catalase activity of the complexes could be established. Kinetic measurements revealed that the catalytic oxidation of 3,5-di-*tert*-butylcatechol catalyzed by **1** shows copper dioxygen chemistry. The forma-

tion of the dicopper dioxygen complex is rate-determining. In the similar reaction catalyzed by **2**, a Michaelis–Menten type kinetics could be observed assuming the formation of a ternary complex. The data show clearly that flexibility and rigidity of the coordinated ligands and the different Cu–Cu interatomic distances exert influence on the reaction rates. Where sterically possible the formation of the dicopper dioxygen is rate-limiting. Further work is in progress in order to disclose the effect of dinuclear complexes on the mechanistic feature of catechol oxidase model systems.

Acknowledgements

We thank the Hungarian Research Fund (OTKA T 030400 and T 043414) for financial support, the French Government for a studentship (KS), and Drs. A. Rockenbauer and L. Korecz for the EPR measurements.

References

[1] M.C. Linder, C. Goode, Biochemistry of Copper, Plenum Press, New York, 1991.
[2] W. Kaim, J. Rall, Angew. Chem. Int. Ed. Engl. 35 (1996) 43.
[3] (a) T.N. Sorrel, Tetrahedron 45 (1989) 3;
(b) N. Kitajima, Y. Moro-oka, J. Chem. Soc., Dalton Trans. (1993) 2665.
[4] N. Kitajima, Y. Moro-oka, Chem. Rev. 94 (1994) 737.
[5] K.D. Karlin, J.D. Hayes, Y. Gultneh, R.W. Cruse, J.W. McKown, J.P. Hutchinson, J. Zubieta, J. Am. Chem. Soc. 106 (1984) 2121.
[6] K.D. Karlin, Y. Gultneh, T. Nicholson, J. Zubieta, Inorg. Chem. 24 (1985) 3727.
[7] R.R. Jacobson, Z. Tyeklar, A. Farooq, K.D. Karlin, S. Liu, J. Zubieta, J. Am. Chem. Soc. 110 (1988) 3690.
[8] Z. Tyeklar, K.D. Karlin, Acc. Chem. Res. 22 (1988) 241.
[9] T. Klabunde, C. Eicken, J.C. Sacchettini, B. Krebs, Nat. Struct. Biol. 5 (1998) 1084.
[10] R. Than, A.A. Feldman, B. Krebs, Coord. Chem. Rev. 182 (1999) 211.
[11] C. Gerdemann, C. Eicken, B. Krebs, Acc. Chem. Res. 35 (2002) 183.
[12] N. Oishi, Y. Nishida, K. Ida, S. Kida, Bull. Chem. Soc. Jpn. 53 (1980) 2847.
[13] M. Réglier, C. Jorand, B. Waegell, J. Chem. Soc., Chem. Commun. (1990) 1752.
[14] B. Srinivas, N. Arulsamy, P.S. Zacharias, Polyhedron 10 (1991) 731.
[15] D.A. Rockcliffe, A.E. Martell, J. Mol. Catal. A 106 (1996) 211.
[16] J. Manzur, A.M. Garcia, V. Rivas, A.M. Atria, J. Valenzuela, E. Spodine, Polyhedron 16 (1997) 2299.
[17] Y.-H. Chung, H.-H. Liu, G.-H. Lee, Y. Wang, J. Chem. Soc., Dalton Trans. (1997) 2825.
[18] E. Monzani, L. Quinti, A. Perotti, L. Casella, M. Gullotti, L. Randaccio, S. Geremia, G. Nardin, P. Faleschini, G. Tabbi, Inorg. Chem. 37 (1998) 553.
[19] F. Zippel, F. Ahlers, R. Werner, W. Haase, H.-F. Nolting, B. Krebs, Inorg. Chem. 35 (1996) 3409.
[20] J. Reim, B. Krebs, J. Chem. Soc., Dalton Trans. (1997) 3793.
[21] P. Gentschev, N. Möller, B. Krebs, Inorg. Chim. Acta 300–302 (2000) 442.
[22] C. Fernandes, A. Neves, A.J. Bortoluzzi, A.S. Mangrich, E. Rentschler, B. Szpoganicz, E. Schwingel, Inorg. Chim. Acta 320 (2001) 12.
[23] A. Neves, L.M. Rossi, A.J. Bortoluzzi, A.S. Mangrich, W. Haase, R. Werner, J. Braz. Chem. Soc. 12 (2001) 747.
[24] S. Torelli, C. Belle, I. Gautier-Luneau, J.L. Pierre, E. Saint-Aman, J.M. Latour, L. Le Pape, D. Luneau, Inorg. Chem. 39 (2000) 3526.
[25] M.R. Malachowski, M.G. Davidson, J.N. Hoffman, Inorg. Chim. Acta 157 (1989) 91.
[26] M.R. Malachowski, M.G. Davidson, Inorg. Chim. Acta 162 (1989) 199.
[27] M.R. Malachowski, H.B. Huynh, L.J. Tomlinson, R.S. Kelly, J.W. Furbeejun, J. Chem. Soc., Dalton Trans. (1995) 31.
[28] M.R. Malachowski, B. Dorsey, J.G. Sackett, R.S. Kelly, A.L. Ferko, R.N. Hardin, Inorg. Chim. Acta 249 (1996) 85.
[29] M.R. Malachowski, J. Carden, M.G. Davidson, W.L. Driessen, J. Reedijk, Inorg. Chim. Acta 257 (1997) 59.
[30] M.T. Malachowski, B.T. Dorsay, M.J. Parker, M.E. Adams, R.S. Kelly, Polyhedron 17 (1998) 1289.
[31] A. Neves, L.M. Rossi, A.J. Bortoluzzi, B. Szpoganicz, C. Wiezbicki, E. Schvingel, Inorg. Chem. 41 (2002) 1788.
[32] G. Speier, J. Mol. Catal. 37 (1986) 259.
[33] J. Kaizer, J. Pap, G. Speier, L. Párkányi, L. Korecz, A. Rockenbauer, J. Inorg. Biochem. 91 (2002) 190.
[34] D.D. Perrin, W.L. Armarego, D.R. Perrin, Purification of Laboratory Chemicals, second ed., Pergamon Press, New York, 1990.
[35] H. Schulze, W. Flaig, Justus Liebigs Ann. Chem. 231 (1952) 575.
[36] R.M. Grienstead, Biochemistry 3 (1964) 1308.
[37] K.D. Karlin, Z. Tyeklár, A. Farooq, M.S. Haka, P. Ghosh, R.W. Cruse, Y. Gultneh, J.C. Hayes, P.J. Toscano, J. Zubieta, Inorg. Chem. 31 (1992) 1436.
[38] Bruker-Nonius Kappa CCD Reference Manual, Nonius B.V., P.O. Box 811, 2600 Av Delft, The Netherlands, 1998.
[39] Z. Otwinowski, W. Minor, in: C.W. Carter Jr., R.M. Sweet (Eds.), Processing of X-Ray Diffraction Data Collected in Oscillation Mode, Academic Press, 1997, New York, Methods Enzymol.: Macromol. Crystallogr. A 276 (1997) 307.
[40] A. Altamore, G. Cascarano, C. Giacovazzo, A. Guagliardi, M.C. Burla, G. Polidori, M. Camalli, J. Appl. Crystallogr. 27 (1994) 435.
[41] G.M Sheldrick, SHELXL-97, Universität Göttingen, 1997.
[42] C.B. Kretschmer, J. Nowakowska, R. Wiebe, Ind. Eng. Chem. 38 (1946) 506.
[43] A.I. Vogel, A Text Book of Quantitative Inorganic Analysis, third ed., Wiley, New York, 1961, p. 343.
[44] A.W. Addison, H.M.J. Hendriks, J. Reedijk, L.K. Thomson, Inorg. Chem. 20 (1981) 103.
[45] K.D. Karlin, I. Sanyal, A. Farooq, R.R. Jacobson, S.N. Shaikh, J. Zubieta, Inorg. Chim. Acta 174 (1990) 13.
[46] K.D. Karlin, J. Shi, J.C. Hayes, J.W. McKown, J.P. Hutchinson, J. Zubieta, Inorg. Chim. Acta 91 (1984) L3.
[47] K.D. Karlin, in: J. Reedijk (Ed.), Bioinorganic Catalysis, second ed., Marcel Dekker, New York, 1999, p. 469.
[48] A.B.P. Lever, E. Milaeva, G. Speier, in: A.B.P. Lever, C.C. Leznoff (Eds.), Phthalocyanines: Principles and Applications, vol. 3, VCH Publishers, New York, 1993, p. 1.
[49] N. Makino, P. McMahill, H.S. Mason, J. Biol. Chem. 249 (1974) 6062.
[50] A.B.P. Lever, Inorganic Electronic Spectroscopy, second ed., Elsevier, Amsterdam, 1984, p. 355.
[51] B.J. Hathaway, Struct. Bond. 57 (1984) 55.
[52] H. Yokoi, Chem. Lett. (1973) 1023.
[53] B.J. Hathaway, in: G. Wilkinson, R.D. Gillard, J.A. McCleverty (Eds.), Comprehensive Coordination Chemistry: the Synthesis, Reactions, Properties and Applications of Coordination Compounds, vol. 5, Pergamon Press, Oxford, 1987, p. 533.
[54] E.I. Solomon, K.W. Penfield, D.E. Wilcox, Struct. Bond. 53 (1983) 1.
[55] P.K. Coughlin, S.J. Lippard, J. Am. Chem. Soc. 103 (1981) 3228.
[56] P.K. Coughlin, S.J. Lippard, J. Am. Chem. Soc. 106 (1984) 2328.

[57] P.L. Burk, J.A. Osborn, M.-T. Youinou, Y. Agnus, R. Louis, R. Weiss, J. Am. Chem. Soc. 103 (1981) 1273.
[58] O. Sénéque, M. Campion, B. Douziech, M. Giorgi, E. Riviére, Y. Journaux, Y.L. Mest, O. Reinaud, Eur. J. Inorg. Chem. (2002) 2007.
[59] W.G. Nigh, in: W.S. Trahanowsky (Ed.), Oxidation in Organic Chemistry. Part B, Academic Press, New York, 1973, p. 1.
[60] M. Lüken, P. Gentschev, N. Möller, J. Anekwe, B. Krebs, in: Proceedings of the 35th International Conference on Coordination Chemistry, Heidelberg, Germany, 2002, p. 315 (Abstract).